Cecal microbiota affects chicken growth performance by regulating fat metabolism

Xiaolong Zhang
Huazhong Agricultural University
Yafang Hu
Huazhong Agricultural University
Abdur Rahman Ansari
Huazhong Agricultural University
Yan Chen
Huazhong Agriculture University
Ranran Cheng
Huazhong Agricultural University
Lei Cui
Huazhong Agricultural University
Abdallah A. Nafady
Huazhong Agricultural University
Abdelmotaleb A. Elokil
Huazhong Agricultural University
El-Sayed M. Abdel-Kafy
Animal production research institute, Agricultural Research Center, Ministry of Agriculture
HUAZHEN LIU (lhz219@mail.hzau.edu.cn)
Huazhong Agricultural University https://orcid.org/0000-0003-1699-8760

Research

Keywords: Chicken, Gut microbiota, Growth performance, Fat metabolism

Posted Date: June 10th, 2020

DOI: https://doi.org/10.21203/rs.3.rs-33862/v1

Abstract

Background

A growing body of evidences suggest critical role of the chicken gut microbiota in growth performance and fat metabolism. However, the underlying mechanism by which the gut microbiota affects chicken growth performance by regulating fat metabolism remains unclear. The purpose of current study was to compare cecal microbial communities between high and low body weight chickens and verify the correlation between fat metabolism and gut microbiota.

Results

Seven-week-old male and female chickens with significantly different body weight were used in the present study. 16S rRNA gene sequencing was used to reveal the cecal microbial community. Fat metabolism levels were compared between high and low body weight chickens. Spearman correlation analysis was used to analyze the relationship between the cecal microbiota and fat metabolism. Transferring fecal microbiota from adult chickens with high body weight into one-day-old chickens was examined by oral administration to verify gut microbiota effects on chicken growth through regulation of fat metabolism. There were significant differences in body weight, chest and leg muscle indexes as well as in cross-sectional area of muscle cells, suggesting different growth performance between high and low body weight chickens. By comparing the relative abundance of gut microbes in the cecal content in high and low body weight chickens, we found that *Microbacterium* and *Sphingomonas* were more abundant in high body weight chickens and *Slackia* was more abundant in low body weight chickens. The fat metabolism level was markedly different in serum, liver, abdominal adipose, chest and leg muscles between high and low body weight chickens. Spearman correlation analysis showed a positive correlation between fat metabolism and the relative abundance of *Microbacterium* and *Sphingomonas* and a negative correlation between fat metabolism and the abundance of *Slackia*. Hence, transferring fecal microbiota, instead of saline, from adult chickens with high body weight into one-day-old chickens improved growth performance and fat metabolism in liver.

Conclusions

These results suggested that cecal microbiota could affect chicken growth performance by regulating fat metabolism.

Background

Gut microbes start to colonize naturally right from the instant of hatching and perhaps even before at the time of egg laying, several microorganisms may get entry through the pores of eggshell [1–3]. Gut microbiota plays an essential role in feed digestibility, nutrient absorption, energy harvest and

metabolism [4, 5]. Intestinal epithelium consists of intestinal epithelial cells (IECs), which creates borderline between the lumen (external environment) and the lamina propria (internal environment) of gut [6, 7]. By keeping pathogenic microbes at bay, the gut IEC-mediated defense system helps in harboring beneficial microbes through sensor and mediator mechanisms in healthy gut [8].

The chicken gastrointestinal tract harbors very complex microbial communities, with the highest bacterial diversity in the cecum [9–13]. Increasingly, studies in chickens have established the importance of the gut microbiota, especially the cecal microbiome, in improving feed digestion, nutrient absorption and growth performance [14–16]. Notably, modification of the gut microbiota using fecal microbiota transplantation [17] or probiotic supplementation [18, 19] as an alternative to antibiotics [20] has been shown to alter chicken growth performance, indicating that the gut microbiota is an important resource for developing natural growth promoters.

Fat metabolism is an important and complex biochemical reaction, including the processes of digestion, absorption, synthesis and catabolism [21]. Digested fat in the form of glycerol and fatty acid is absorbed into the bloodstream and transported to the liver, adipose tissue and other organs [22, 23]. Fat synthesized in the liver is bound to apolipoprotein or cholesterol to form very-low-density lipoprotein (VLDL), which is transported in blood to other tissues for storage or usage [24]. However, fat synthesized in adipose tissue is stored there. Balanced fat metabolism can improve host growth performance and meat quality, yet imbalanced fat metabolism results in obesity and disease. Recent investigations have suggested that the gut microbiota is an important environmental factor affecting energy harvest from the diet and energy storage in mammals, and these studies have focused on the relationship between the gut microbiota and obesity [25–27]. Other studies of chickens have shown that the gut microbiota plays a key role in regulating fat metabolism [28, 29].

According to the World Health Organization (WHO) and the Food and Agriculture Organization (FAO), probiotics are termed as “live microorganisms which when administered in adequate amounts confer a health benefit for the host” [8, 30]. Invasion of probiotic alters the proteolytic activity and bacterial metabolism of short chain fatty acids (SCFA) and amino acids in mouse gut [31]. However, little is known about whether the intervention of probiotics affects chicken growth performance by regulating fat metabolism. Therefore, in the present study, cecal microbial communities and fat metabolism levels were compared between high and low body weight chickens and fecal microbiota transplantation was also used to verify the correlation between fat metabolism and gut microbiota.

Results

Growth performance was different between high and low body weight chickens

There were significant differences in the body weight ($P < 0.001$) (Fig. 1A), chest muscle index ($P < 0.01$) (Fig. 1B) and leg muscle index ($P < 0.05$) (Fig. 1C) between high and low body weight chickens. Hematoxylin and eosin (HE) staining results showed that the average cross-sectional areas of chest muscle cells (Fig. 1D) and leg muscle cells (Fig. 1E) were significantly larger in high than in low body

weight chickens ($P < 0.05$). These results suggested that there was a significant difference in growth performance between high and low body weight chickens.

Differences in cecal microbiota in high and low body weight chickens

The microbial diversity and composition in cecal content of high and low body weight chickens were analyzed by 16S rRNA gene sequencing. The results showed no significant differences in microbial diversity or relative abundances in content between high and low body weight chickens (Fig. 2A-B). Beta diversity showed some separation between high and low body weight groups (Fig. 2C). At the phylum level, *Firmicutes*, *Bacteroidetes* and *Proteobacteria* were the most abundant phyla. The relative abundance of *Firmicutes* was lower, and the relative abundance of *Bacteroidetes* was higher in high body weight chickens (Fig. 2D). The ratio of *Firmicutes* to *Bacteroidetes* was lower in high body weight chickens (Fig. 2E). At the genus level, *Bacteroides* was the dominant genus in cecal content (Fig. 2F). Linear discriminant analysis effect size (LEfSe) analysis showed that the relative abundances of *Faecalibacterium, Microbacterium*, *Slackia*, and *Sphingomonas* were significantly different in high and low body weight chickens (Fig. 2G). Phylogenetic investigation of communities by reconstruction of unobserved states (PICRUSt) analysis showed that PPAR signaling pathway was significantly different in cecal contents between high and low body weight chickens (Fig. 2H).

Fat metabolism in liver differed between high and low body weight chickens

HE staining results showed that there was more vacuolar fat in the liver of high body weight chickens (Fig. 3A), while the expressions of fat synthesis-related genes including cytochrome P450 2C45 (CYP2C45), fatty acid desaturase 1 (FADS1) and acyl-CoA synthetase long chain family member 1 (ACSL1) (Fig. 3B) and the fat catabolism-related genes fasting-induced adipose factor (fiaf), peroxisome proliferator-activated receptor alpha (PPARα) and carnitine palmitoyl transferase I (CPT-1) (Fig. 3C) were significantly higher in the livers of high body weight chickens than in low body weight chickens ($P < 0.05$). The expression of fat synthesis-related genes acetyl CoA carboxylase (ACC) and fatty acid synthase (FAS) was higher in high body weight chickens as compared to low body weight chickens, but not significantly. The expression of fat transport related gene including apolipoprotein A-I (ApoAI) was significantly higher in the liver of high body weight chickens than in low body weight chickens ($P < 0.05$) (Fig. 3D). Immunohistochemistry (IHC) staining showed that phosphor-AMP-activated protein kinase (P-AMPK) was mainly distributed in the cytoplasm and nucleus of hepatocytes in liver tissue (Fig. 3E), and the protein expression of P-AMPK was much higher in high body weight chickens than that in low body weight chickens ($P < 0.01$) (Fig. 3F). Western blot results also showed a higher protein expression of P-AMPK in high body weight chickens ($P < 0.01$) (Fig. 3G-I).

Fat metabolism level in blood and abdominal adipose differed between high and low body weight chickens

In abdominal adipose, HE staining results showed that adipocytes were vacuolar, the number of adipocytes in abdominal adipose tissue in high body weight chickens was significantly higher than in low

body weight chickens ($P < 0.05$) (Fig. 4A), and the average diameter of adipocytes was significantly smaller in high than in low body weight chickens ($P < 0.05$) (Fig. 4B). In serum, the concentration of high-density lipoprotein cholesterol (HDL-C) in high body weight chickens was significantly higher than in low body weight chickens ($P < 0.05$). The concentration of low-density lipoprotein cholesterol (LDL-C) was significantly lower in high than in low body weight chickens ($P < 0.05$). There were no significant differences in the concentrations of triglyceride (TG) or total cholesterol (TC) between high and low body weight chickens (Fig. 4C). q-PCR results showed that the expression levels of ACC and FAS were lower in high body weight chickens than those in low body weight chickens, but there were no significant differences (Fig. 4D). The expression levels of adipocyte differentiation-related genes, including sterol regulatory element-binding protein 1 (SREBP1) and adiponectin, were significantly lower in high body weight chickens ($P < 0.05$), and adipocyte protein 2 (AP2) and peroxisome proliferator-activated receptor gamma (PPARG) were also lower in high body weight chickens, but there were no significant differences (Fig. 4E).

Fat metabolism level in muscle differed between high and low body weight chickens

Compared with the low body weight chickens, expression of the fat synthesis-related gene ACC was lower in chest muscle and leg muscle of high body weight chickens (Fig. 5A), the expression of the fat transport-related gene adipocyte fatty acid binding protein (A-FABP) was much lower in the chest muscle of high body weight chickens ($P < 0.01$) (Fig. 5B), and the expression of the fat catabolism-related gene CPT-1 was significantly higher in the chest and leg muscle of high body weight chickens ($P < 0.05$) (Fig. 5C). IHC results showed that P-AMPK was mainly distributed in the connective tissue of chest and leg muscle, and the protein expression of P-AMPK was significantly higher in chest muscle (Fig. 5D) and leg muscle (Fig. 5E) of high body weight chickens ($P < 0.05$). Western blot results also showed higher expression of P-AMPK in chest muscle (Fig. 5F-G) and leg muscle (Fig. 5H-I).

Differential cecal microbiota was related to fat metabolism in chickens

Spearman correlation analysis was used to analyze the correlation between fat metabolism and the differential cecal microbiota. The results showed that the abundance of *Sphingomonas* and *Microbacterium* was significantly positively correlated with fat metabolism in serum, liver, chest muscle and leg muscle. The abundance of *Slackia* was significantly negatively correlated with the fat metabolism in serum, liver, chest muscle and leg muscle (Fig. 6).

Fecal microbiota transplantation improved growth performance and fat metabolism level in liver

Fecal microbiota transplantation (FMT) was performed to investigate the effect of gut microbiota on growth performance and fat metabolism. The results showed that the body weight in FMT group was significantly higher than that in control group ($p < 0.05$) (Fig. 7A). The expressions of fat synthesis-related gene (Fig. 7B), fat catabolism-related gene (Fig. 7C), and fat transport-related gene (Fig. 7D) in liver were significantly up-regulated ($p < 0.05$).

Discussion

Growing body of evidence shows that use of antibiotics as feed additives in poultry production is increasing to enhance growth performance. Nevertheless, long-term use of antibiotics can produce antibiotic-resistant zoonotic pathogens and cause antibiotic residues in food [32, 33]. Furthermore, poorly absorbed antibiotics are excreted unchanged in feces and urine, resulting in environmental pollution [34]. Therefore, many countries have banned the use of antibiotics as a growth promoter [35, 36]. Consequently, the development of alternatives to antibiotic growth promoters (AGPs) is an important issue in animal production and food safety.

Herein, transferring of fecal microbiota from adult chickens with high body weight into one-day-old chickens was examined by oral administration to verify gut microbiota effects on chicken growth through regulation of fat metabolism. Blood biochemical indicators are closely related to fat metabolism and have been used as criteria to select lean chicken lines [37]. In the present study, the concentration of serum HDL-C was significantly higher in high body weight chickens, suggesting that higher HDL-C in high body weight chickens may effectively carry cholesterol in blood and transport it to the liver [38, 39]. The liver is the largest solid organ and plays a critical role in lipid metabolism, providing significant energy resources for host growth [40, 41]. High body weight chickens exhibited higher expression of fat synthesis-related genes in the liver, as well as greater numbers of fat vacuoles in hepatocytes, suggesting stronger fat synthesis in the livers of high body weight chickens. At the same time, the expression of fat catabolism-related genes increased, ultimately promoting the oxidative catabolism of fatty acids, thereby providing energy for the growth and development of chickens [42–44]. Abdominal adipose tissue is the main organ of fat synthesis and deposition; the upregulated expression of adipocyte differentiation-related genes can mediate excessive proliferation and differentiation of adipocytes, causing excessive deposition of fat in animal bodies [45]. In the present study, the expression of fat synthesis- and adipocyte differentiation-related genes in low body weight chickens was significantly higher than in high body weight chickens, increasing fat synthesis in abdominal adipose tissue. Moreover, the average diameter of adipocytes in low body weight chickens was much larger indicating that more synthesized fat was stored in abdominal adipose tissue in low body weight chickens. As a result, excessive fat deposition affected growth performance [45]. These results indicate that the differential fat metabolism level is the key factor leading to differences in growth performance.

The composition of the gut microbiota is closely related to fat metabolism in mammals and chickens [28, 29, 46, 47]. The gut microbiota can ferment indigestible dietary components and thereby produce short-chain fatty acids, which regulate energy homeostasis and metabolism, the functions of adipose tissue, skeletal muscle and liver tissue [48, 49]. Further findings indicated that *Firmicutes* and *Bacteroidetes* can induce fat deposition, and the higher ratio of *Firmicutes* to *Bacteroidetes*, the greater is the fat storage [50–53]. In the present study, the ratio of *Firmicutes* to *Bacteroidetes* was lower in high body weight chickens. Taken together with the fat metabolism results, high body weight chickens store less fat, yet degrade fat to obtain more energy to improve growth [48, 49]. Gut microbiota affect fat synthesis and deposition in animals by regulating the expression of fat metabolism-related genes in tissues [44, 54, 55].

Herein, Spearman analysis demonstrated positive correlations between HDL-C, CPT-1 and P-AMPK and the relative abundances of *Sphingomonas* and *Microbacterium*. While negative correlations between HDL-C, CPT-1, and P-AMPK and the relative abundance of *Slackia*, indicating that *Sphingomonas* and *Microbacterium* may promote the oxidative decomposition of fatty acids to stimulate growth and development of animals, yet *Slackia* promoted the deposition of fat in animals. Hence, transferring fecal microbiota, instead of saline, from adult chickens with high body weight into one-day-old chickens improved the growth performance and fat metabolism in liver.

Conclusions

In summary, the level of fat metabolism differs between high and low body weight chickens. *Sphingomonas, Microbacterium* and *Slackia* in the cecal contents can regulate fat metabolism in the liver, abdominal adipose tissue, chest muscle and leg muscle, thus affecting the growth performance of chickens. These findings provide novel insights into the role of the cecal microbiota in fat metabolism and growth performance of chickens and contribute to the development of alternatives to AGPs for improving chicken production efficiency.

Methods

Animals

The Institutional Animal Care and Use Committee of Huazhong Agricultural University approved all the animal procedures and all methods were performed in accordance with the relevant guidelines and regulations.

Newly hatched chickens were reared under similar husbandry conditions and were fed a corn-soybean, pathogen free diet in pellet form in a poultry farming with no medication or vaccination. The birds had *ad libitum* access of water and feed. When they were 7 weeks old, male and female chickens (n=10) with high or low body weight chickens were selected for next study. For fecal microbiota transplantation, adult high body weight chickens were selected as donors and one-day-old chickens (n=30) with the same genetic background were selected as recipients. The recipients were randomly divided into two groups: saline control group (group C) and fecal microbiota transplantation group (group FMT). Fecal bacteria were transplanted every day by oral administration for four weeks.

Samples collection

After being fasted 12 hours, the chickens were sacrificed. Blood, liver and abdominal adipose were harvested. Chest muscle and leg muscle were collected and weighed. To ensure the comparability of research results, the same part of each organ was chosen for next analysis. For gut microbiota analysis, the contents of the ceca from the selected twenty chickens were snap frozen in liquid nitrogen and stored at -80°C. For histo-morphological analysis, freshly harvested chest muscle, leg muscle, and liver tissues were fixed in 4% paraformaldehyde solution; abdominal adipose tissues from each chicken were fixed in

optimal cutting temperature (OCT). For the molecular studies and gene expression analysis, the parts of freshly harvested muscle, adipose and liver tissues were snap frozen in liquid nitrogen and then stored at -80°C. For blood biochemical parameters analysis, blood samples from birds were centrifuged at 1500 × g for 15 min and serum was snap frozen in liquid nitrogen and stored at -80°C.

Muscle index calculation

The muscle index was calculated using the following formula: muscle index=muscle weight (g)/body weight (g).

Microbial genomic DNA extraction and 16S rRNA gene sequencing

16S rRNA sequencing was used to compare the microbial composition between high and low body weight chickens. Total bacterial genomic DNA samples were extracted using Fast DNA SPIN extraction kits (MP Biomedicals, Santa Ana, CA, USA), following the manufacturer's instructions, and stored at -20°C prior to further analysis. The quantity and quality of extracted DNA fragments were measured using a NanoDrop ND-1000 spectrophotometer (Thermo Fisher Scientific, Waltham, MA, USA) and agarose gel electrophoresis, respectively.

PCR amplification of the bacterial 16S rRNA gene V3-V4 region was performed using the forward primer 338F (5'-ACTCCTACGGGAGGCAGCA-3') and the reverse primer 806R (5'-GGACTACHVGGGTWTCTAAT-3'). Sample-specific 7-bp barcodes were incorporated into the primers for multiplex sequencing. The PCR components contained 5 μl of Q5 reaction buffer (5×), 5 μl of Q5 High-Fidelity GC buffer (5×), 0.25 μl of Q5 High-Fidelity DNA Polymerase (5 U/μl), 2 μl (2.5 mM) of dNTPs, 1 μl (10 μM) of each forward and reverse primer, 2 μl of DNA Template, and 8.75 μl of dd H_2O. Thermal cycling consisted of initial denaturation at 98 °C for 2 min, followed by 25 cycles consisting of denaturation at 98 °C for 15 s, annealing at 55 °C for 30 s, and extension at 72 °C for 30 s, with a final extension of 5 min at 72 °C. PCR amplicons were purified with Agencourt AMPure Beads (Beckman Coulter, Indianapolis, IN) and quantified using the PicoGreen dsDNA Assay Kit (Invitrogen, Carlsbad, CA, USA). After the individual quantification step, amplicons were pooled in equal amounts, and paired-end 2×300 bp sequencing was performed using the Illumina MiSeq platform with the MiSeq Reagent Kit v3 at Shanghai Personal Biotechnology Co., Ltd. (Shanghai, China).

Sequencing data analysis

The Quantitative Insights Into Microbial Ecology (QIIME, v1.8.0) pipeline was employed to process the sequencing data, as previously described [56]. Briefly, raw sequencing reads with exact matches to the barcodes were assigned to respective samples and identified as valid sequences. The low-quality sequences were filtered through the following criteria [57, 58]: sequences that had a length of <150 bp, sequences that had average Phred scores of <20, sequences that contained ambiguous bases, and sequences that contained mononucleotide repeats of >8 bp. Paired-end reads were assembled using FLASH [59]. After chimera detection, the remaining high-quality sequences were clustered into operational

taxonomic units (OTUs) at 97% sequence identity by UCLUST [60]. A representative sequence was selected from each OTU using default parameters. OTU taxonomic classification was conducted by BLAST searching the representative sequences set against the Greengenes Database [61] using the best hit [62]. An OTU table was further generated to record the abundance of each OTU in each sample and the taxonomy of these OTUs. OTUs containing less than 0.001% of total sequences across all samples were discarded. To minimize the difference in sequencing depth across samples, an averaged, rounded rarefied OTU table was generated by averaging 100 evenly resampled OTU subsets under 90% of the minimum sequencing depth for further analysis.

Blood biochemical parameters analysis

To test the fat metabolism level in blood, the concentrations of serum TG, TC, HDL-C and LDL-C were determined using a Rayto Chemistry Analyzer Chemray 240 (Chemray 240, China) according to the commercial diagnostic kits' instructions.

Hematoxylin and eosin staining

To compare the morphological changes, liver, chest muscle, and leg muscle tissue samples embedded in paraffin were cut into 3-μm-thick sections. Abdominal adipose tissue samples fixed in OCT were cut into 10-μm-thick sections. HE staining was performed using a routine protocol, and the examination of stained tissue sections was accomplished by light microscopy (Olympus BX51, Tokyo, Japan) with a digital camera (DP72; Olympus). The average diameter of adipocytes and the average areas of chest muscle cells and leg muscle cells were quantitated using Image Pro Plus 6.0.

Immunohistochemical staining

To test the distribution and protein expression of P-AMPK, immunohistochemical staining was performed following the same steps as described in earlier studies [63, 64]. Briefly, the tissue sections were deparaffinized twice in xylene and rehydrated in a graded series of ethanol. A microwave oven (MYA-2270M, Haier, Qingdao, China) was used for heat antigen retrieval in citrate acid buffer solution (pH 6.0) for 20 minutes (5 minutes at high level, i.e., 700 W, and 15 minutes at low level, i.e., 116 W). After cooling at room temperature for 2-3 h, 3% H_2O_2 was used to block endogenous peroxidase. For blocking of nonspecific antibody binding, the tissue sections were incubated with 5% bovine serum albumin (BSA) at 37 °C for 30 minutes. Sections were then incubated with primary antibodies using rabbit anti-P-AMPK antibody (1:100) (Cell Signaling Technology, Inc., USA). Subsequently, tissue sections were incubated at 37 °C with suitable horseradish peroxidase (HRP)-conjugated secondary antibodies (Boster, Wuhan, China) for 30 minutes. Immunostaining for all the tissue sections was accomplished using the chromogenic marker diaminobenzidine (DAB) (Boster, Wuhan, China), and counterstaining was performed using hematoxylin. Finally, the sections were washed, dried, dehydrated, cleared, and finally mounted with a coverslip.

Serial sections were examined under a light microscope (BH-2; Olympus, Japan) with a digital camera (DP72; Olympus), and the fields of vision were chosen according to different regions of the liver and muscle tissue in each section. The distributions and expression levels of different proteins were measured in high-power fields selected at random. All of the images were taken using the same microscope and camera set. Image-Pro Plus (IPP) 6.0 software (Media Cybernetics, USA) was used to calculate the mean density for positive staining.

Western blotting

To test the protein expression of P-AMPK, western blotting was performed following previously described methods [65]. Briefly, the frozen specimens were powdered in liquid nitrogen and homogenized in lysis buffer with a protease inhibitor. The supernatants were vortexed, incubated on ice and centrifuged at 12,000 × g for 5 min. Protein concentrations were measured using the BCA protein quantification kit (Beyotime, Jiangsu, China). Equal amounts of total proteins (40 μg) were subjected to 10% sodium dodecyl sulfate-polyacrylamide gel electrophoresis (SDS-PAGE) (30 min at 80 volts, and after that 80 min at 120 volts). Then, the separated proteins were transferred onto a polyvinylidene difluoride (PVDF) membrane (Merck Millipore, USA). The membranes were incubated with rabbit anti-P-AMPK (1:1000) (Cell Signaling Technology, Inc., USA), rabbit anti-AMPK (1:1000) (ABclonal, China), mouse anti-GAPDH (1:10000) (Proteintech Group, Inc., USA) and rabbit anti-β-actin (1:5000) (ABclonal, China) antibodies for 12 h. After washing in 1X TBST buffer three times, samples were incubated with peroxidase-conjugated secondary antibody (1:5000) for 120 min (Boster, China). The blots were developed with Super Signal West Pico Chemiluminescent Substrate (Thermo Fisher Scientific, Waltham, MA, USA) and visualized using ChemiDoc-It™ Imaging System. Western blot results were analyzed using IPP 6.0 software.

Real-time quantitative polymerase chain reaction (Q-PCR)

To measure the expression of fat metabolism-related genes at the mRNA level, total RNA was isolated from the liver, abdominal adipose tissue, chest muscle and leg muscle with Trizol reagent (Takara, Japan) according to the manufacturer's instructions. The cDNA was synthesized using the RevertAid First Strand cDNA Synthesis Kit (Takara, Japan). The reaction mixture (10 μl) for qPCR contained 5 μL of SYBR Select Master Mix for CFX (Takara, Japan), 0.4 μL of each forward and reverse primer, 3.2 μL of ddH_2O and 1 μL of template cDNA. The Q-PCR reactions were performed on a Bio-Rad CFX Connect real-time Q-PCR detection system.

Table 1
Primers used for real-time Q-PCR

Gene	Primer sequences (5′ to 3′)	Accession No.
β-actin	f-TTGTTGACAATGGCTCCGGT	NM_205518.1
	r-TCTGGGCTTCATCACCAACG	
ACC	f-TCCAGCAGAACCGCATTGACAC	NM_205505.1
	r-GTATGAGCAGGCAGGACTTGGC	
FAS	f-GCTCTGCGTCTGCTTCAGTCTAC	NM_001199487.1
	r-GGTACAGGACTCTGCCATCAATGC	
FADS1	f-CCGTGCCACTGTGGAGAAGATG	LC061145.1
	r-GCCTAGAAGCAACGCAGAGAAGAG	
CYP2C45	f-AACAAGCACCACCACACGATACG	AJ430583.1
	r-GGTCAGCCACGCAAGGTCTTC	
ACSL1	f-GACTAATGGTCACAGGAGCAGCAC	NM_001012578.1
	r-CCAGGCATTGACAGTGAGCATCC	
PPARα	f-TGCTGTGGAGATCGTCCTGGTC	AF163809.1
	r-CTGTGACAAGTTGCCGGAGGTC	
CPT-1	f-GCCAAGTCGCTCGCTGATGAC	DQ314726.1
	r-ACGCCTCGTAGGTCAGACAGAAC	
fiaf	f-AGATCAAGCAGCAGCAGTACAAGC	XM_001232283.5
	r-ACGCTCACATTATGGCTCTGGTTG	
A-FABP	f-ACAATGGCACACTGAAGCAGG	FJ493543.1
	r-AGCAGGTTCCCATCCACCAC	
SREBP1	f-GGTCCGGGCCATGTTGA	AJ310768.1
	r-CAGGTTGGTGCGGGTGA	
PPARG	f-GAATGCCACAAGCGGAGAAGGAG	NM_001001460.1
	r-GCTCGCAGATCAGCAGATTCAGG	
AP2	f-ACTGAAGCAGGTGCAGAAGTGG	NM_204290.1
	r-TGCATTCCACCAGCAGGTTCC	
Adiponectin	f-TACGTGTACCGCTCCGCCTTC	KP729052.1

Gene	Primer sequences (5′ to 3′)	Accession No.
	r-GTGCTGCTGTCGTAGTGGTTCTG	

(Bio-Rad, Hercules, CA, USA). The Q-PCR conditions were as follows: predenaturation at 95 °C for 5 min, followed by 40 cycles of denaturation at 95 °C for 30 s, annealing at 60 °C for 30 s, and elongation at 72 °C for 20 s. The primer sequences are listed in Table 1. β-Actin was chosen as a reference for Q-PCR. All samples were run in triplicate, and gene expression levels were quantified using the ΔΔCt method.

Statistical analysis

Sequence data analyses were mainly performed using QIIME and R packages (v3.2.0). OTU-level alpha diversity indexes, such as the Chao richness index and Shannon diversity index, were calculated using the OTU table in QIIME. The taxonomy compositions and abundances were visualized using Excel. LEfSe was performed to detect differentially abundant taxa across groups using the default parameters (LDA>2) [66]. Based on high-quality sequences, microbial functions were predicted by PICRUSt, [67]. The significant differences between pairs of samples or among multiple groups of KEGG pathways were visualized using the STAMP software package. Spearman's correlations between the gut microbiota and fat metabolism were determined using the R software package. All data are presented as the means ± standard error of mean (SEM). All analyses and graphic representations were performed with Prism software 5.01 (GraphPad Software, Inc., San Diego, USA). The statistical significance of the mean values in two-group comparisons was determined using Student's t-test. A p value <0.05 was considered statistically significant.

Abbreviations

AGPs: Antibiotic growth promoters; HE: Hematoxylin and eosin; HDL-C: High- density lipoprotein cholesterol; LDL-C: Low-density lipoprotein cholesterol; TG: Triglyceride; TC: Total cholesterol; FADS1: Fatty acid desaturase 1; CYP2C45: Cytochrome P 450 2C45; ACSL1: Acyl-CoA synthetase long chain family member 1; PPARα: Peroxisome proliferator-activated receptor alpha; CPT-1: Carnitine palmitoyl transferase I; fiaf: Fasting-induced adipose factor; ACC: Acetyl CoA carboxylase; FAS: Fatty acid synthase; IHC: Immunohistochemistry; P-AMPK: Phosphor-AMP-activated protein kinase; SRESP1: Sterol regulatory element-binding protein 1; AP2: Adipocyte protein 2; PPARG: Peroxisome proliferator-activated receptor gamma; A-FABP: Adipocyte fatty acid binding protein; LEfSe: Linear discriminant analysis effect size; PICRUSt: Phylogenetic investigation of communities by reconstruction of unobserved states; VLDL: Very low-density lipoprotein; OCT: Optimal cutting temperature; BSA: Bovine serum albumin; DAB: Diaminobenzidine; IPP: Image-Pro Plus; SDS-PAGE: Sodium dodecyl sulfate-polyacrylamide gel electrophoresis; PVDF: polyvinylidene difluoride; Q-PCR: Quantitative polymerase chain reaction; QIIME: Quantitative Insights Into Microbial Ecology; OTUs: Operational taxonomic units; SD: Standard deviation

Declarations

Ethics approval and consent to participate

The current scientific investigation was conducted in accordance with the rules and regulations of the ethics committee for use of animals, Huazhong Agricultural University (HZAU), Wuhan, China.

Consent for publication

Not applicable.

Availability of data and materials

The raw 16S rRNA gene sequencing data are available at the NCBI Sequence Read Archive (SRA), under BioProject PRJNA637407.

Competing interests

The authors declare that they have no conflicts of interest.

Funding

The National Key Research and Development Program of China (2017YFE0113700), the Hubei Provincial Natural Science Foundation of China (2017CFB514), and the National Natural Science Foundation of China (30800808) supported this work.

Authors' contributions

XL Zhang, YF Hu and HZ Liu designed the research. XL Zhang, YF Hu, Y Chen, RR Cheng, L Cui, and AA Nafady performed the research. XL Zhang, YF Hu, AA Elokil and HZ Liu analyzed the data. XL Zhang, YF Hu, AR Ansari, El-SM Abdel-Kafy and HZ Liu wrote the paper with the help of all authors. All authors read and approved the final version of the manuscript.

Acknowledgments

We sincerely thank Xinyun Li and Yunlong Ma for their suggestions and revisions on this manuscript and Shijun Li for his assistance in animal management and sample collections.

References

1. Roto SM, Kwon YM, Ricke SC. Applications of in ovo technique for the optimal development of the gastrointestinal tract and the potential influence on the establishment of its microbiome in poultry. Fron Vet Sci. 2016;3:63.
2. Lee S, La T-M, Lee H-J, Choi I-S, Song C-S, Park S-Y, Lee J-B, Lee S-W. Characterization of microbial communities in the chicken oviduct and the origin of chicken embryo gut microbiota. Sci Rep. 2019;9:1–11.

3. Carrasco JMD, Casanova NA, Miyakawa MEF. Microbiota, Gut Health and Chicken Productivity. What Is the Connection? Microorganisms. 2019;7.
4. Fetissov SO. Role of the gut microbiota in host appetite control: bacterial growth to animal feeding behaviour. Nat Re Endocrinol. 2017;13:11.
5. Parkar SG, Kalsbeek A, Cheeseman JF. Potential role for the gut microbiota in modulating host circadian rhythms and metabolic health. Microorganisms. 2019;7:41.
6. Fan H, Wang A, Wang Y, Sun Y, Han J, Chen W, Wang S, Wu Y, Lu Y. Innate Lymphoid Cells. Regulators of Gut Barrier Function and Immune Homeostasis. J Immunol Res. 2019;2525984; doi:10.1155/2019/2525984.
7. Peterson LW, Artis D. Intestinal epithelial cells: regulators of barrier function and immune homeostasis. Nat Rev Immunol. 2014;14:141–53.
8. Wan ML, Ling K, El-Nezami H, Wang M. Influence of functional food components on gut health. Crit Rev Food Sci Nutr. 2019;59:1927–36.
9. Wei S, Morrison M, Yu Z. Bacterial census of poultry intestinal microbiome. Poult Sci. 2013;92:671–83.
10. Bjerrum L, Engberg RM, Leser TD, Jensen BB, Finster K, Pedersen K. Microbial community composition of the ileum and cecum of broiler chickens as revealed by molecular and culture-based techniques. Poult Sci. 2006;85:1151–64.
11. Saxena S, Saxena VK, Tomar S, Sapcota D, Gonmei G. Characterisation of caecum and crop microbiota of Indian indigenous chicken targeting multiple hypervariable regions within 16S rRNA gene. Br Poult Sci. 2016;57:381–9.
12. Awad WA, Mann E, Dzieciol M, Hess C, Schmitz-Esser S, Wagner M, Hess M. Age-Related Differences in the Luminal and Mucosa-Associated Gut Microbiome of Broiler Chickens and Shifts Associated with Campylobacter jejuni Infection. Front Cell Infect Microbiol. 2016;6:154. doi:10.3389/fcimb.2016.00154.
13. Pandit RJ, Hinsu AT, Patel NV, Koringa PG, Jakhesara SJ, Thakkar JR, Shah TM, Limon G, Psifidi A, Guitian J, et al. Microbial diversity and community composition of caecal microbiota in commercial and indigenous Indian chickens determined using 16 s rDNA amplicon sequencing. Microbiome. 2018;6:115.
14. Stanley D, Hughes RJ, Geier MS, Moore RJ. Bacteria within the Gastrointestinal Tract Microbiota Correlated with Improved Growth and Feed Conversion: Challenges Presented for the Identification of Performance Enhancing Probiotic Bacteria. Front Microbiol. 2016;7:187. doi:10.3389/fmicb.2016.00187.
15. Stanley D, Hughes RJ, Moore RJ. Microbiota of the chicken gastrointestinal tract: influence on health, productivity and disease. Appl Microbiol Biotechnol. 2014;98:4301–10.
16. Yan W, Sun C, Yuan J, Yang N. Gut metagenomic analysis reveals prominent roles of Lactobacillus and cecal microbiota in chicken feed efficiency. Sci Rep. 2017;7:45308. doi:10.1038/srep45308.

17. Siegerstetter SC, Petri RM, Magowan E, Lawlor PG, Zebeli Q, O'Connell NE, Metzler-Zebeli BU. Fecal Microbiota Transplant from Highly Feed-Efficient Donors Shows Little Effect on Age-Related Changes in Feed-Efficiency-Associated Fecal Microbiota from Chickens. Appl Environ Microbiol. 2018;84:e02330-17. doi:10.1128/AEM.02330-17.
18. Videvall E, Song SJ, Bensch HM, Strandh M, Engelbrecht A, Serfontein N, Hellgren O, Olivier A, Cloete S, Knight R. Major shifts in gut microbiota during development and its relationship to growth in ostriches. Mol Ecol. 2019;28:2653–67.
19. Angelakis E. Weight gain by gut microbiota manipulation in productive animals. Microb Pathog. 2017;106:162–70.
20. Yadav S, Jha R. Strategies to modulate the intestinal microbiota and their effects on nutrient utilization, performance, and health of poultry. J Anim Sci Biotechnol. 2019;10:1–11.
21. D'Aquila T, Hung Y-H, Carreiro A, Buhman KK. Recent discoveries on absorption of dietary fat. Presence, synthesis, and metabolism of cytoplasmic lipid droplets within enterocytes. Biochim Biophys Acta Mol Cell Biol Lipids. 2016;1861:730–47.
22. Hermier D. Lipoprotein metabolism and fattening in poultry. J Nutr. 1997;127(Suppl 5):805–8. doi:10.1093/jn/127.5.805S.
23. Margetak C, Travis G, Entz T, Mir PS, Wei S, Dodson MV. Fatty Acid Composition of Phospholipids and in the Central and External Positions of Triacylglycerol in Muscle and Subcutaneous Fat of Beef Steers Fed Diets Supplemented with Oil Containing n6 and n3 Fatty Acids While Undergoing One of Three 48 h Feed Withdrawal Treatments. J Lipids. 2012;2012:543784. doi:10.1155/2012/543784.
24. Alves-Bezerra M, Cohen DE. Triglyceride Metabolism in the Liver. Compr Physiol. 2017;8:1–8. doi:10.1002/cphy.c170012.
25. Backhed F, Ding H, Wang T, Hooper LV, Koh GY, Nagy A, Semenkovich CF, Gordon JI. The gut microbiota as an environmental factor that regulates fat storage. Proc Natl Acad Sci U S A. 2004;101:15718–23.
26. Wang Y, Kuang Z, Yu X, Ruhn KA, Kubo M, Hooper LV. The intestinal microbiota regulates body composition through NFIL3 and the circadian clock. Science. 2017;357:912–6.
27. Turnbaugh PJ, Ley RE, Mahowald MA, Magrini V, Mardis ER, Gordon JI. An obesity-associated gut microbiome with increased capacity for energy harvest. Nature. 2006;444:1027–31.
28. Yang J, Qian K, Zhang W, Xu Y, Wu Y. Effects of chromium-enriched bacillus subtilis KT260179 supplementation on chicken growth performance, plasma lipid parameters, tissue chromium levels, cecal bacterial composition and breast meat quality. Lipids Health Dis. 2016;15:188. doi:10.1186/s12944-016-0355-8.
29. Wen C, Yan W, Sun C, Ji C, Zhou Q, Zhang D, Zheng J, Yang N. The gut microbiota is largely independent of host genetics in regulating fat deposition in chickens. ISME J. 2019;13:1422–36. doi:10.1038/s41396-019-0367-2.
30. Mountzouris KC, Kotzampassi K, Tsirtsikos P, Kapoutzis K, Fegeros K. Effects of Lactobacillus acidophilus on gut microflora metabolic biomarkers in fed and fasted rats. Clin Nutr. 2009:28:318–

24.

31. Martin FPJ, Wang Y, Sprenger N, Yap IK, Lundstedt T, Lek P, Rezzi S, Ramadan Z, Van Bladeren P, Fay LB. Probiotic modulation of symbiotic gut microbial–host metabolic interactions in a humanized microbiome mouse model. Mol Sys Biol. 2008;4:157. doi:10.1038/msb4100190.
32. Allen HK, Trachsel J, Looft T, Casey TA. Finding alternatives to antibiotics. Ann N Y Acad Sci. 2014;1323:91–100.
33. Pamer EG. Resurrecting the intestinal microbiota to combat antibiotic-resistant pathogens. Science. 2016;352:535–8.
34. Joy SR, Li X, Snow DD, Gilley JE, Woodbury B, Bartelt-Hunt SL. Fate of antimicrobials and antimicrobial resistance genes in simulated swine manure storage. Sci Total Environ. 2014;481:69–74.
35. Casewell M, Friis C, Marco E, McMullin P, Phillips I. The European ban on growth-promoting antibiotics and emerging consequences for human and animal health. J Antimicrob Chemother. 2003;52:159–61.
36. Hoese A, Clay SA, Clay DE, Oswald J, Trooien T, Thaler R, Carlson CG. Chlortetracycline and tylosin runoff from soils treated with antimicrobial containing manure. J Environ Sci Health B. 2009;44:371–8.
37. Zhang HL, Xu ZQ, Yang LL, Wang YX, Li YM, Dong JQ, Zhang XY, Jiang XY, Jiang XF, Li H, et al. Genetic parameters for the prediction of abdominal fat traits using blood biochemical indicators in broilers. Br Poult Sci. 2018;59:28–33.
38. Oldoni F, Sinke RJ, Kuivenhoven JA. Mendelian disorders of high-density lipoprotein metabolism. Circ Res. 2014;114:124–42.
39. Manthei KA, Yang SM, Baljinnyam B, Chang L, Glukhova A, Yuan W, Freeman LA, Maloney DJ, Schwendeman A, Remaley AT, et al. Molecular basis for activation of lecithin:cholesterol acyltransferase by a compound that increases HDL cholesterol. eLife. 2018;7:e41604. doi:10.7554/eLife.41604.
40. Grijalva J, Vakili K. Neonatal liver physiology. Semin Pediatr Surg. 2013;22:185–9.
41. Parry SA, Hodson L. Influence of dietary macronutrients on liver fat accumulation and metabolism. J Investig Med. 2017;65:1102–15.
42. Witczak CA, Sharoff CG, Goodyear LJ. AMP-activated protein kinase in skeletal muscle: from structure and localization to its role as a master regulator of cellular metabolism. Cell Mol Life Sci. 2008;65:3737–55.
43. Niu Y, Yuan H, Fu L. Aerobic exercise's reversal of insulin resistance by activating AMPKalpha-ACC-CPT1 signaling in the skeletal muscle of C57BL/6 mice. Int J Sport Nutr Exerc Metab. 2010;20:370–80.
44. Kim DH, Jeong D, Kang IB, Kim H, Song KY, Seo KH. Dual function of Lactobacillus kefiri DH5 in preventing high-fat-diet-induced obesity: direct reduction of cholesterol and upregulation of PPAR-alpha in adipose tissue. Mol Nutr Food Res. 2017;61:1700252. doi:10.1002/mnfr.201700252.

45. Xiao Y, Kong F, Xiang Y, Zhou W, Wang J, Yang H, Zhang G, Zhao J. Comparative biogeography of the gut microbiome between Jinhua and Landrace pigs. Sci Rep. 2018;8:5985. doi:10.1038/s41598-018-24289-z.
46. Ridaura VK, Faith JJ, Rey FE, Cheng J, Duncan AE, Kau AL, Griffin NW, Lombard V, Henrissat B, Bain JR, et al. Gut microbiota from twins discordant for obesity modulate metabolism in mice. Science. 2013;341:1241214. doi:10.1126/science.1241214.
47. Pascale A, Marchesi N, Govoni S, Coppola A, Gazzaruso C. The role of gut microbiota in obesity, diabetes mellitus, and effect of metformin: new insights into old diseases. Curr Opin Pharmacol. 2019;49:1–5.
48. Canfora EE, Jocken JW, Blaak EE. Short-chain fatty acids in control of body weight and insulin sensitivity. Nat Rev Endocrinol. 2015;11:577–91.
49. Hu J, Lin S, Zheng B, Cheung PCK. Short-chain fatty acids in control of energy metabolism. Crit Rev Food Sci Nutr. 2018;58:1243–49.
50. Ley RE, Turnbaugh PJ, Klein S, Gordon JI. Microbial ecology: human gut microbes associated with obesity. Nature. 2006;444:1022–23.
51. Koliada A, Syzenko G, Moseiko V, Budovska L, Puchkov K, Perederiy V, Gavalko Y, Dorofeyev A, Romanenko M, Tkach S, et al. Association between body mass index and Firmicutes/Bacteroidetes ratio in an adult Ukrainian population. BMC Microbiol. 2017;17:120.
52. Compare D, Rocco A, Sanduzzi Zamparelli M, Nardone G. The Gut Bacteria-Driven Obesity Development. Dig Dis. 2016;34:221–9.
53. Indiani C, Rizzardi KF, Castelo PM, Ferraz LFC, Darrieux M, Parisotto TM. Childhood Obesity and Firmicutes/Bacteroidetes Ratio in the Gut Microbiota: A Systematic Review. Child Obes. 2018;14:501–9.
54. Lunedo R, Furlan LR, Fernandez-Alarcon MF, Squassoni GH, Campos DMB, Perondi D, Macari M. Intestinal microbiota of broilers submitted to feeding restriction and its relationship to hepatic metabolism and fat mass: Fast-growing strain. J Anim Physiol Anim Nutr. 2019;103:1070–80.
55. Alves CC, Waitzberg DL, de Andrade LS, Dos Santos Aguiar L, Reis MB, Guanabara CC, Junior OA, Ribeiro DA, Sala P. Prebiotic and Synbiotic Modifications of Beta Oxidation and Lipogenic Gene Expression after Experimental Hypercholesterolemia in Rat Liver. Front Microbiol. 2010;2017:8. doi:10.3389/fmicb.2017.02010.
56. Caporaso JG, Kuczynski J, Stombaugh J, Bittinger K, Bushman FD, Costello EK, Fierer N, Pena AG, Goodrich JK, Gordon JI, et al. QIIME allows analysis of high-throughput community sequencing data. Nat Methods. 2010;7:335–6.
57. Gill SR, Pop M, Deboy RT, Eckburg PB, Turnbaugh PJ, Samuel BS, Gordon JI, Relman DA, Fraser-Liggett CM, Nelson KE. Metagenomic analysis of the human distal gut microbiome. Science. 2006;312:1355–9.
58. Chen H, Jiang W. Application of high-throughput sequencing in understanding human oral microbiome related with health and disease. Front Microbiol. 2014;5:508.

doi:10.3389/fmicb.2014.00508.

59. Magoc T, Salzberg SL. FLASH fast length adjustment of short reads to improve genome assemblies. Bioinformatics. 2011;27:2957–63.
60. Edgar RC. Search and clustering orders of magnitude faster than BLAST. Bioinformatics. 2010;26:2460–61.
61. DeSantis TZ, Hugenholtz P, Larsen N, Rojas M, Brodie EL, Keller K, Huber T, Dalevi D, Hu P, Andersen GL. Greengenes, a chimera-checked 16S rRNA gene database and workbench compatible with ARB. Appl Environ Microbiol. 2006;72:5069–72.
62. Altschul SF, Madden TL, Schaffer AA, Zhang J, Zhang Z, Miller W, Lipman DJ. Gapped BLAST and PSI-BLAST: a new generation of protein database search programs. Nucleic Acids Res. 1997;25:3389–402.
63. Ansari AR, Ge X-H, Huang H-B, Huang X-Y, Zhao X, Peng K-M, Zhong J-M, Liu H-Z. Effects of lipopolysaccharide on the histomorphology and expression of toll-like receptor 4 in the chicken trachea and lung. Avian Pathol. 2016;45:530–7.
64. Ansari AR, Ge X-H, Huang H-B, Wang J-X, Peng K-M, Yu M, Liu H-Z. Expression patterns of Toll-Like receptor 4 in pig uterus during pregnancy. Pak Vet J. 2015;35:466–9.
65. Hnasko TS, Hnasko RM. The western blot. In: ELISA. Humana Press: New York; 2015. p. 87–96.
66. Segata N, Izard J, Waldron L, Gevers D, Miropolsky L, Garrett WS, Huttenhower C. Metagenomic biomarker discovery and explanation. Genome Biol. 2011;12:R60. doi:10.1186/gb-2011-12-6-r60.
67. Langille MG, Zaneveld J, Caporaso JG, McDonald D, Knights D, Reyes JA, Clemente JC, Burkepile DE, Vega Thurber RL, Knight R, et al. Predictive functional profiling of microbial communities using 16S rRNA marker gene sequences. Nat Biotechnol. 2013;31:814–21.

Figures

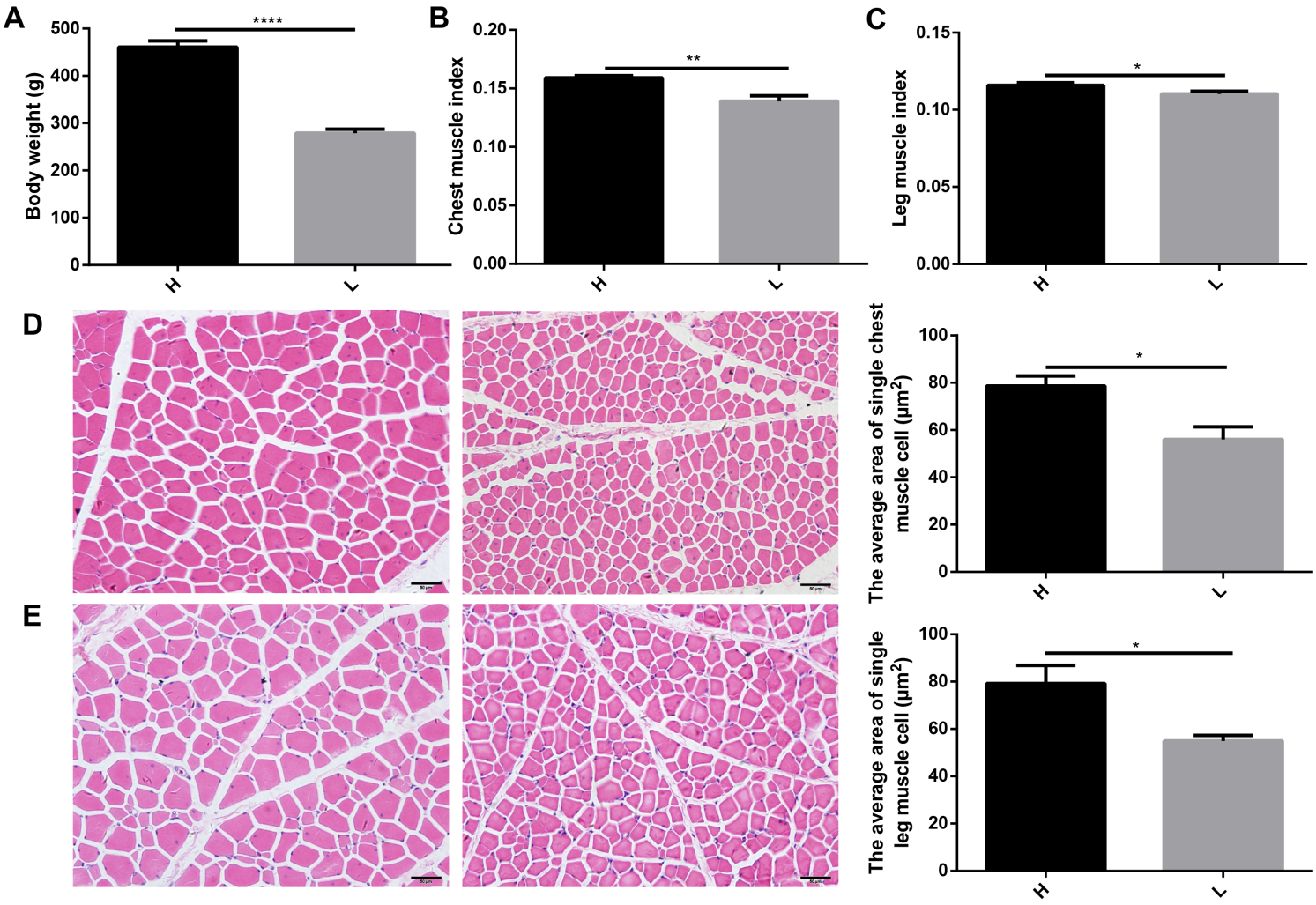

Figure 1

Different growth performance between high and low body weight chickens. (A) Body weight. (B) Chest muscle index. (C) Leg muscle index. (D) Section of chest muscle with H&E staining and the comparison of single cell's cross-sectional area. (E) Section of leg muscle with H&E staining and the comparison of single cell's cross-sectional area. H represents high body weight chickens and L represents low body weight chickens. Scale bars = 50μm. All data are presented as the means ± SEM. P values were calculated using Student's t-test, *p<0.05, **p<0.01, ***p<0.001, ****p<0.0001.

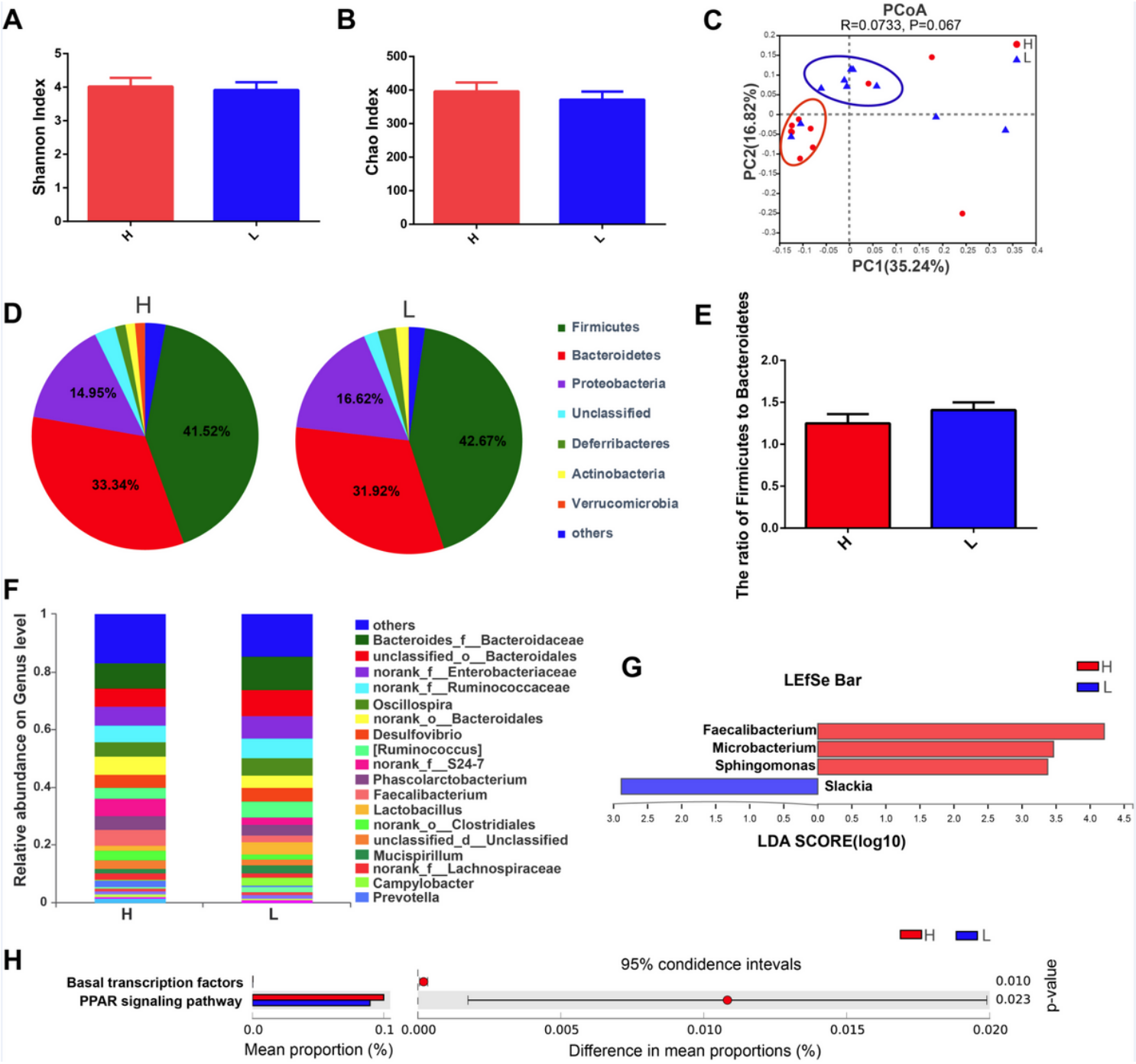

Figure 2

Differences in cecal microbiota between high and low body weight chickens. (A) Microbial community diversity (measured by the Shannon index). (B) Microbial community abundance (measured by the Chao index). (C) Beta diversity of high and low body weight chickens. (D) The composition of microbial communities at the phylum level. (E) The ratio of Firmicutes to Bacteroidetes. (F) The composition of microbial communities at the phylum level. (G) LDA score for LEfSe analysis. (H) Predicted function of cecal microbiota. The comparison third level of KEGG pathways were shown in the post-hoc plot.

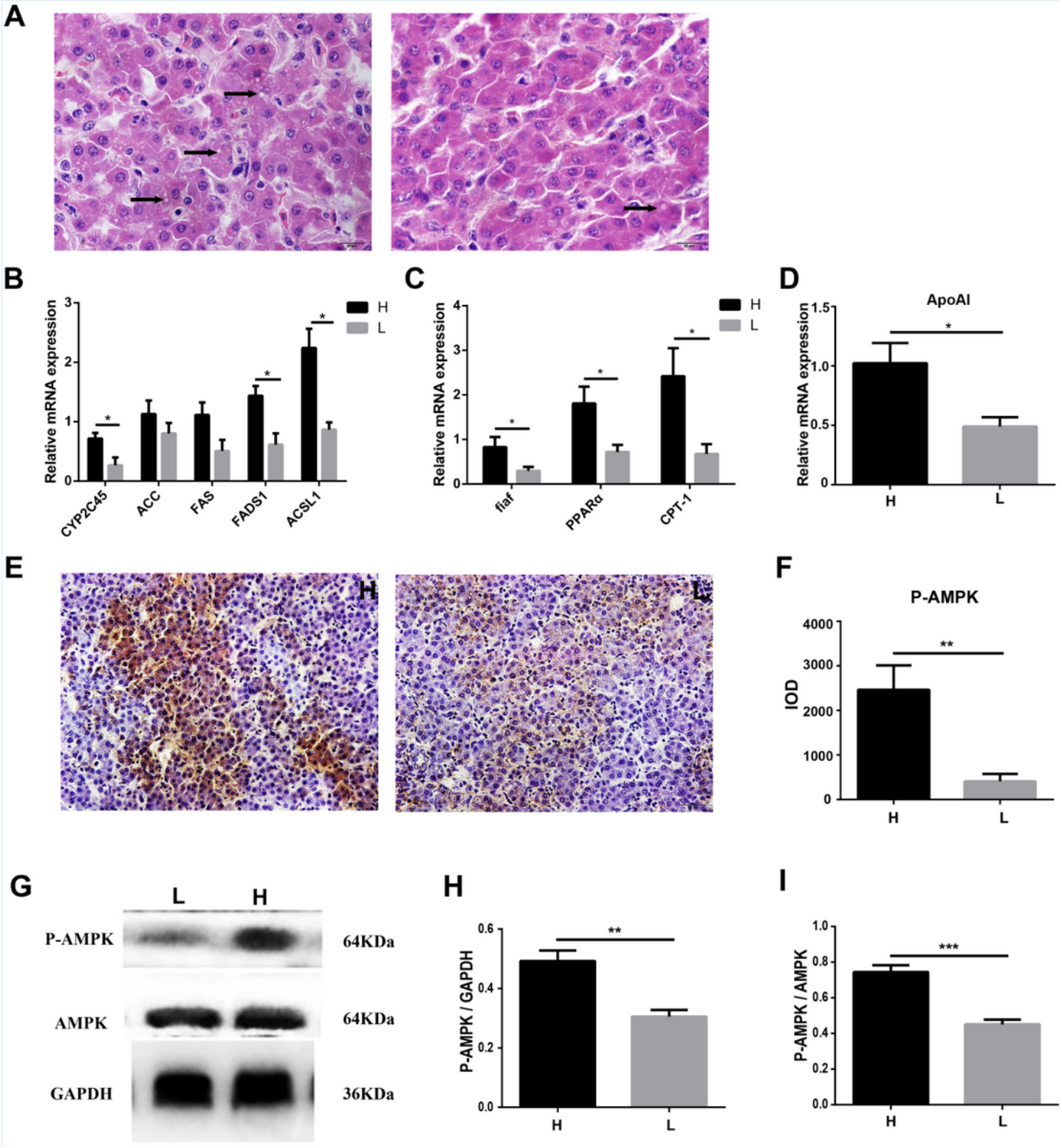

Figure 3

Differences of fat metabolism levels in liver between high and low body weight chickens. (A) Fat content of hepatocytes (HE staining). The white dots indicated by the arrows in the figure are fat droplets. (B) The expression of fat anabolism-related genes (Q-PCR). (C) The expression of fat catabolism-related genes (Q-PCR). (D) The expression of fat transport related genes (Q-PCR). (E) The distribution of P-AMPK (IHC). The arrows in the figure indicate positive expression of P-AMPK. (F) IOD comparison of IHC. (G-I) The

protein expression of P-AMPK (western blot). Scale bars = 50μm. All data are presented as the means ± SEM. P values were calculated using Student's t-test, *p<0.05, **p<0.01.

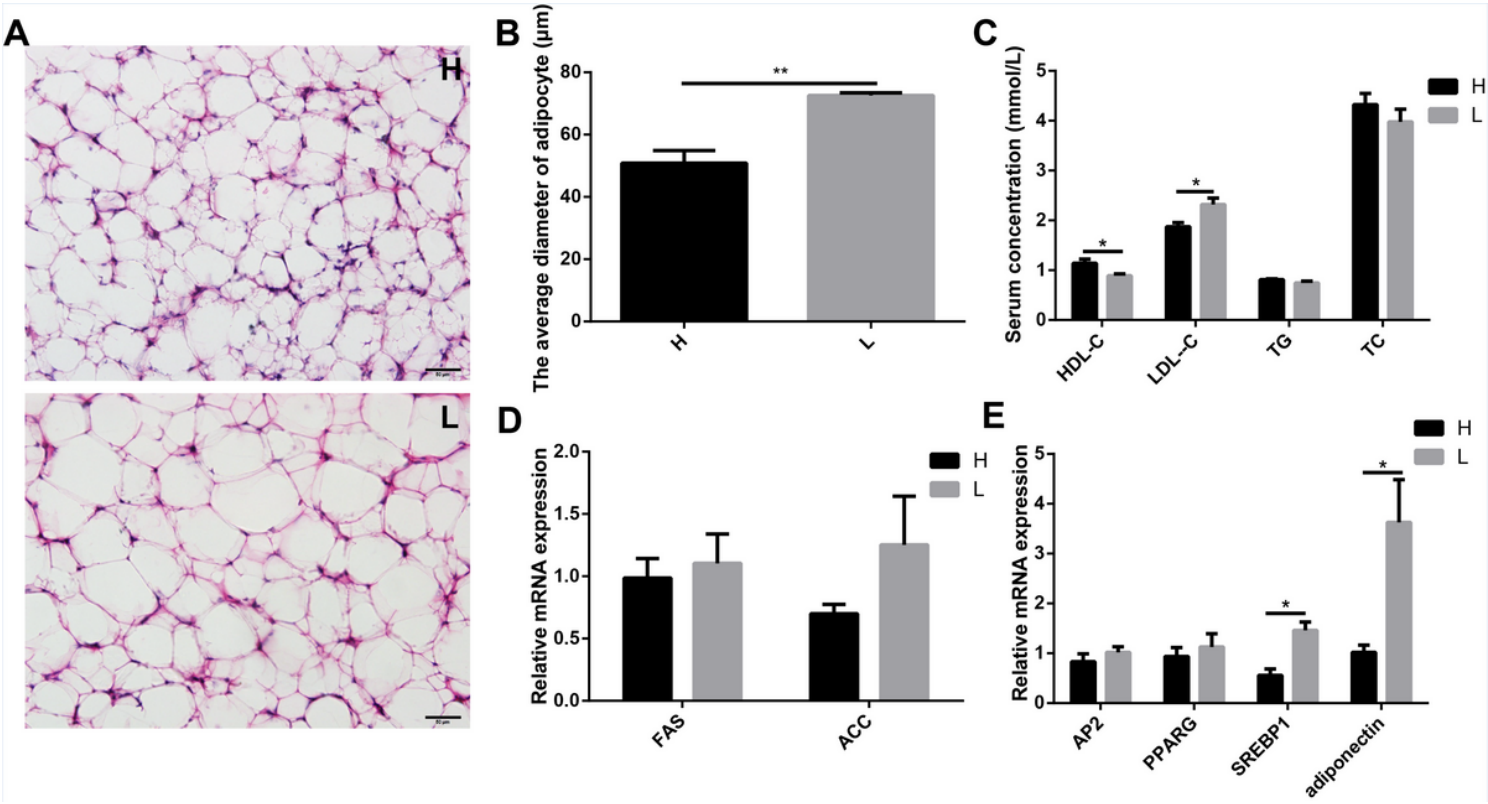

Figure 4

Different fat metabolism levels in blood and abdominal adipose tissue. (A) Different adipocyte structure by HE staining. (B) The average diameter of adipocyte. (C) Different blood biochemical parameters related to lipid metabolism. (D) The expression of fat anabolism-related genes (Q-PCR). (E) The expression of adipocyte differentiation-related genes. Scale bars = 50μm. All data are presented as the means ± SEM. P values were calculated using Student's t-test, *p<0.05, **p<0.01.

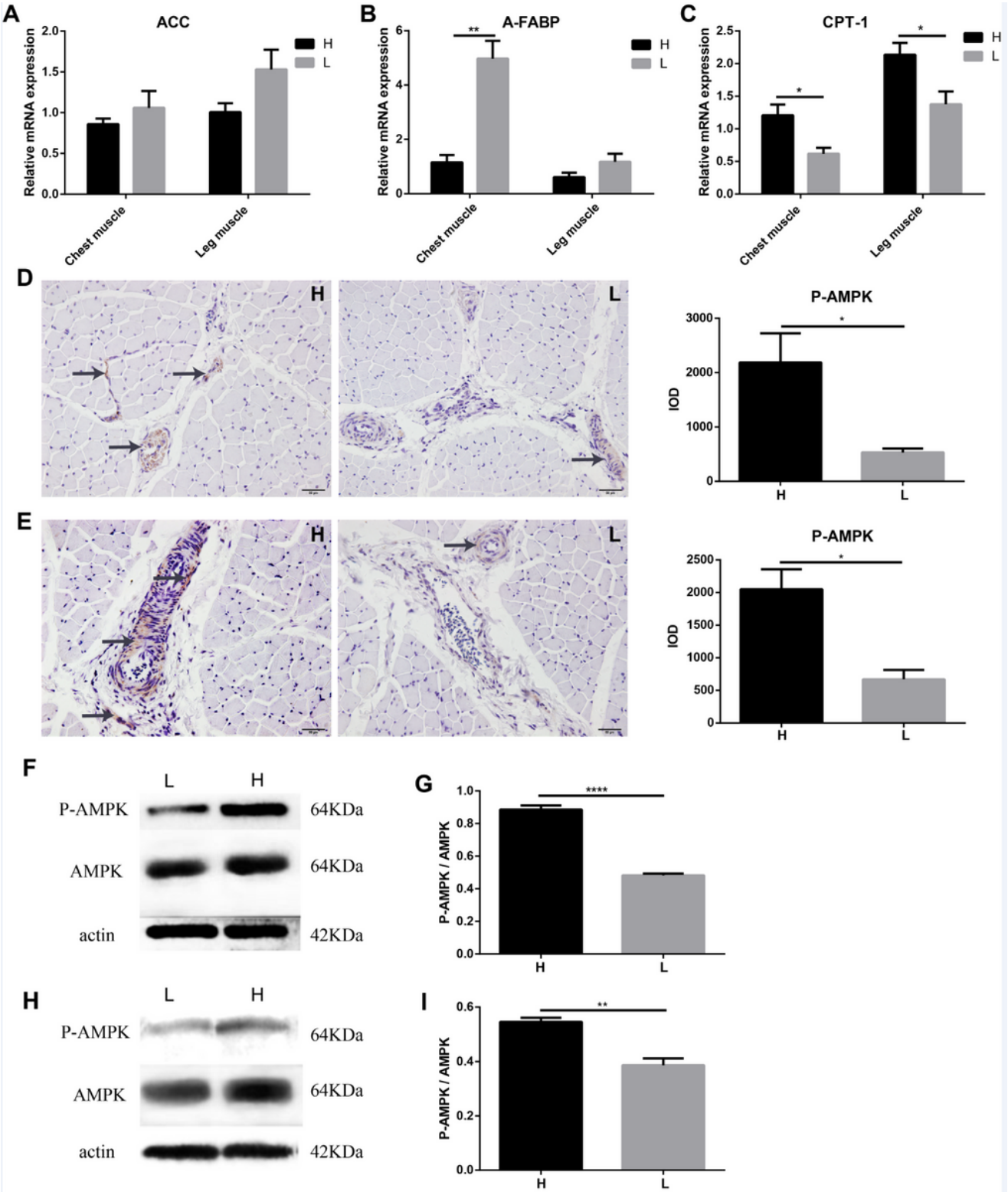

Figure 5

Different fat metabolism levels in muscle tissues. (A) The expression of fat anabolism-related genes (Q-PCR). (B) The expression of fat transport-related genes (Q-PCR). (C) The expression of fat catabolism-related genes (Q-PCR). (D) The distribution and protein expression of P-AMPK in chest muscle (IHC). (E) The distribution and protein expression of P-AMPK in leg muscle (IHC). The arrows in the figures indicate positive signals. (F-G) The protein expression of P-AMPK in chest muscle (western blot). (H-I) The protein

expression of P-AMPK in leg muscle (western blot). H represents high body weight chickens and L represents low body weight chickens. Scale bars = 50μm. All data are presented as the means ± SEM. P values were calculated using Student's t-test, *p<0.05, **p<0.01.

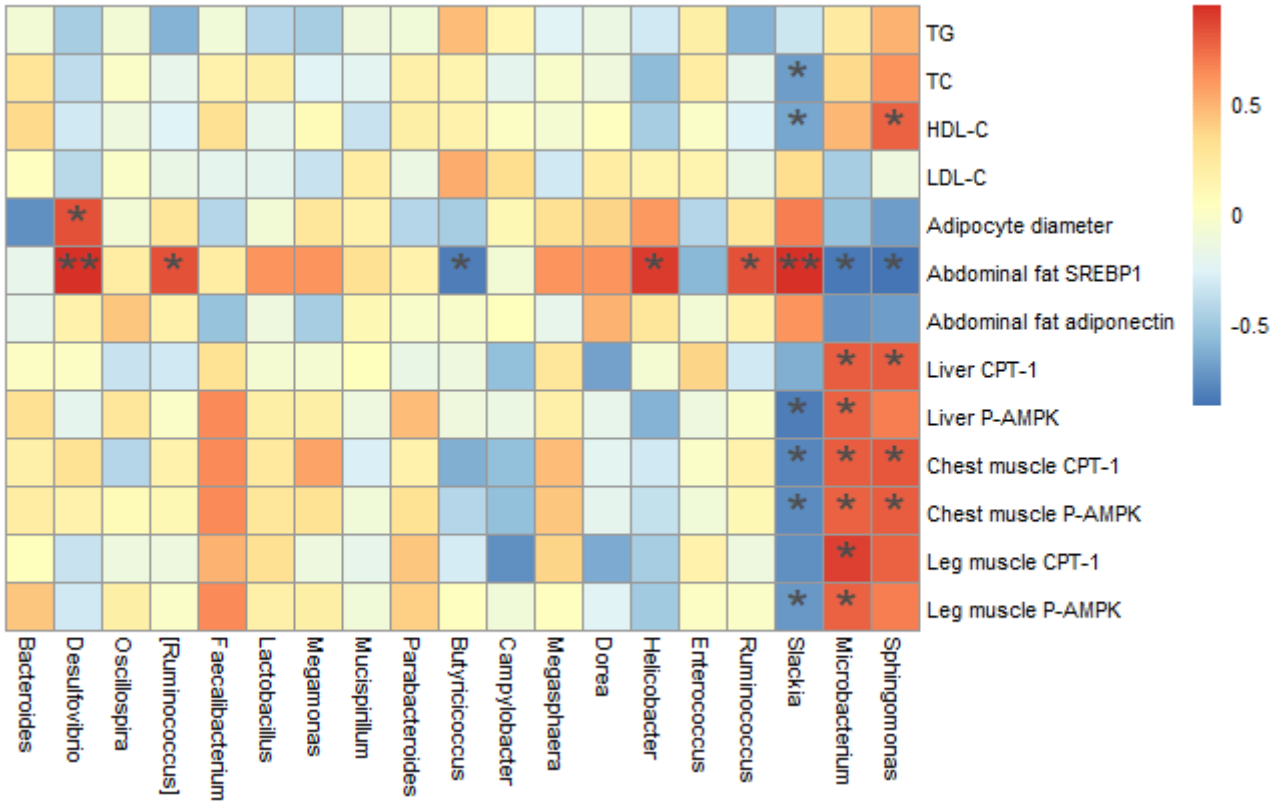

Figure 6

Heatmap of Spearman's correlations between cecal microbe abundance and fat metabolism. The colors range from blue (negative correlation) to red (positive correlation). P values were calculated using Student's t-test, *p< 0.05 and **p< 0.01.

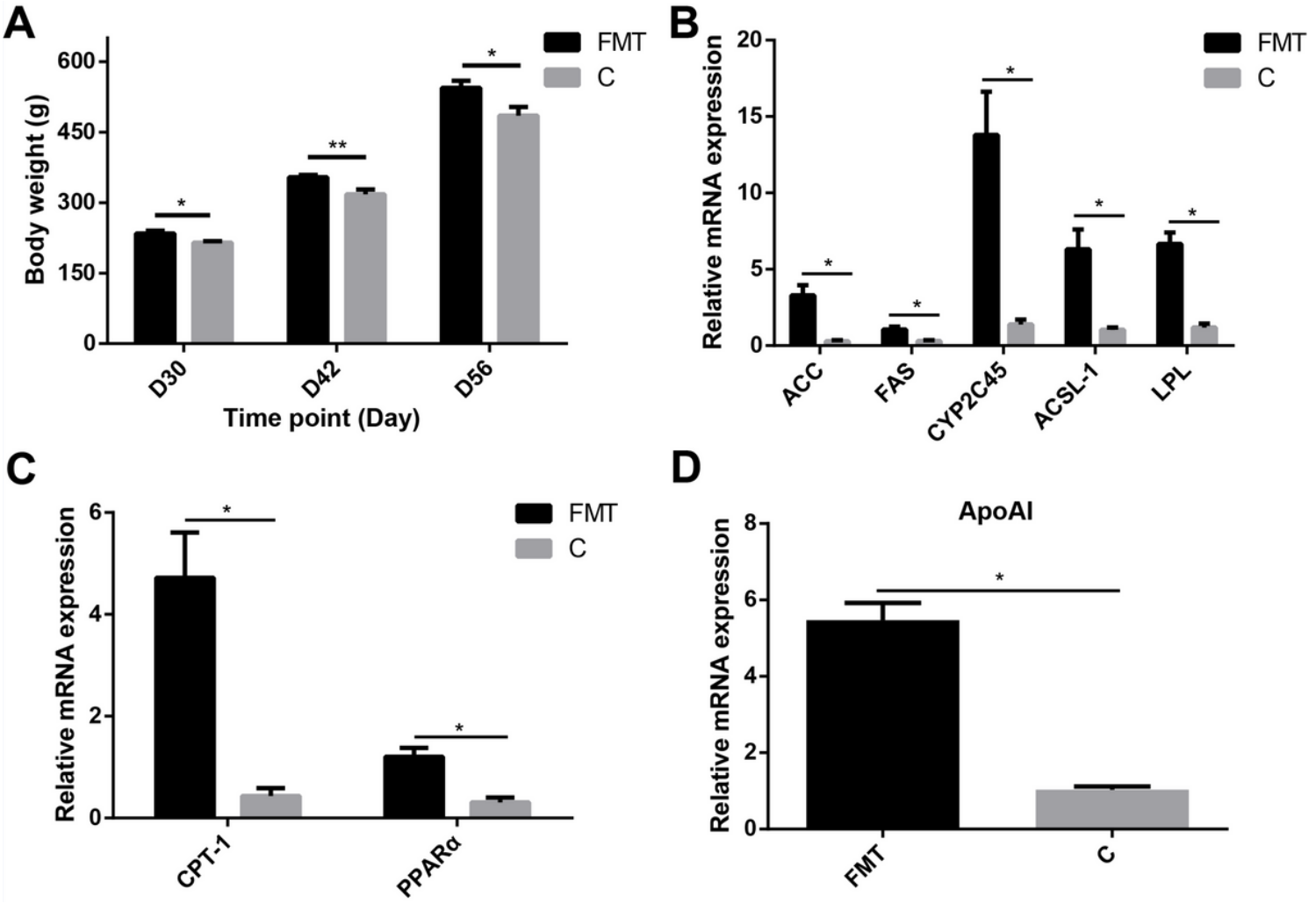

Figure 7

FMT influence growth performance and fat metabolism level in liver. (A) Comparison of body weight between C and FMT group. (B) The expression of fat anabolism-related genes (Q-PCR). (C) The expression of fat catabolism-related genes (Q-PCR). (D) Expression of fat transport related genes (Q-PCR). All data are presented as the means ± SEM. P values were calculated using Student's t-test, *p<0.05, **p<0.01.